Rodriguez-Sanchez, M. R., Sanchez-Gonzalez, A., Marugan-Cruz, C. & Santana, D. (2015). Flow patterns of external solar receivers. *Solar Energy*, 122, pp. 940–953.

DOI: 10.1016/j.solener.2015.10.025

Flow patterns of external solar receivers

M.R. Rodriguez-Sanchez[1*], A. Sanchez-Gonzalez[1], C. Marugan-Cruz[1], D. Santana[1].

[1] Department of Fluids and Thermal Engineering. Carlos III University of Madrid.

Av. Universidad 30, Leganés, 28911 Madrid (Spain)

*Phone number: +34 916246034, Fax: +34916249430, e-mail:

mrrsanch@ing.uc3m.es

Abstract

The design of flow paths of solar-central external-receiver with molten salt as heat transfer fluid is crucial to increase the solar plant availability and for the secure receiver operation with respect to the material failure. The parameters that most affect the start-up and shut-down of the receiver are the direct normal irradiance, the sun elevation angle, and the ambient conditions. In addition, the limits of the feed-pump system and the minimum turbulent Reynolds number also limit the hours of operation to avoid receiver damage. Under nominal conditions of operation the most influential factors are the film temperature, the thermal stresses and the pressure drop.

In this study, a whole year range of operation has been analysed. Different flow pattern configurations have been simulated including simple or multiple flow paths. In the latter case it has been also studied configurations including crossover between flow paths. The analysis of the different configurations has been done based on thermal, mechanical and hydrodynamics limits in order to increase the global efficiency of the power plant. In view of the results special attention has to be paid to the crossover to equalise the solar flux that reaches both flow paths in the start-up and shut-down. However, to maintain good levels of thermal efficiency close to midday it is more important a good distribution of the solar flux than get a flux balance between paths.

The configuration that maximizes the thermal efficiency includes two flow paths in which the flow configuration varies along the day: one crossover just before the middle of the path in the sunrise and sunset, and none crossover for high solar flux. If the configuration of crossovers cannot be varied, it is recommended to avoid the use of crossovers in the receiver.

Keywords

External solar central receiver; Molten salt; Flow pattern; Crossover.

Nomenclature

DNI : Direct Normal Insolation. [W/m^2]

HTF : Heat Transfer Fluid.

SPT : Solar Power Tower.

UTS : Ultimate tensile strength.

Symbols

Cp : Specific heat. [J/kg °C]

C : Flux density on the receiver. [-]

N : Number of elements. [-]

Nu : Nusselt number. [-]

Pr : Prandtl number. [-]

Re : Reynolds number. [-]

S : Surface area. [m^2]

T : Temperature. [°C]

$\dot{Q}$: Heat power. [W]

dt : Tube diameter. [m]

f : Petukhov coefficient. [-]

$\dot{m}$: Mass flow. [kg/s]

v : Salt velocity. [m/s]

Greek letters

ΔP : Pressure drop. [Pa]

ε : Nusselt coefficient for transition regime. [-]

η : Receiver thermal efficiency. [-]

μ : Dynamic viscosity. [Pa/s]

ρ : Salt density. [kg/m^3]

σ : Thermal stress. [Pa]

Subscripts

amb : Ambient.

$film$: Film.

fp : Flow path.

in : Inlet.

int : Internal.

l : Laminar.

$\min$: Minimum.

p : Panel.

rec : Receiver.

$salt$: Salt.

t : Turbulent

$tubes$: Tubes.

we : External wall.

1. Introduction

In Solar Power Tower (SPT) the solar direct irradiation is concentrated on the receiver by thousands of individually sun-tracking mirrors to reach peak solar flux, up to 1 MW/m^2 (Lata et al., 2008). In the receiver the radiation energy is transferred by conduction and convection to the heat transfer fluid (HTF) reaching high temperatures that allows to generate electricity in a power block.

The external central receiver is placed at the top of a tower, configured as a 360º cylindrical tubular receiver, formed by panels made of thin walled tubes. The HTF follows a serpentine path, passing through adjacent panels. The flow pattern of each receiver can vary with the ambient conditions and operation requirements (see Figure 1). Wagner (Wagner, 2008) analysed eight simple flow configurations that have been employed in the design software System Advisor Model of NREL (SAM, 2015). Figure 1 shows different configurations, notice that Figures 1.5 to 1.8 are composed by a single flow path in which the whole HTF flows through all the panels of the receiver (note that the inlet and the outlet of the receiver are in adjacent panels of the northern or southern side), whereas Figures 1.1 to 1.4 have two symmetric flow paths, and half HTF mass only flows through one half of the panels, from north to south or from south to north. In addition, both paths could be crossed one time (Figures 1.1 and 1.2) or none (Figures 1.3 and 1.4).

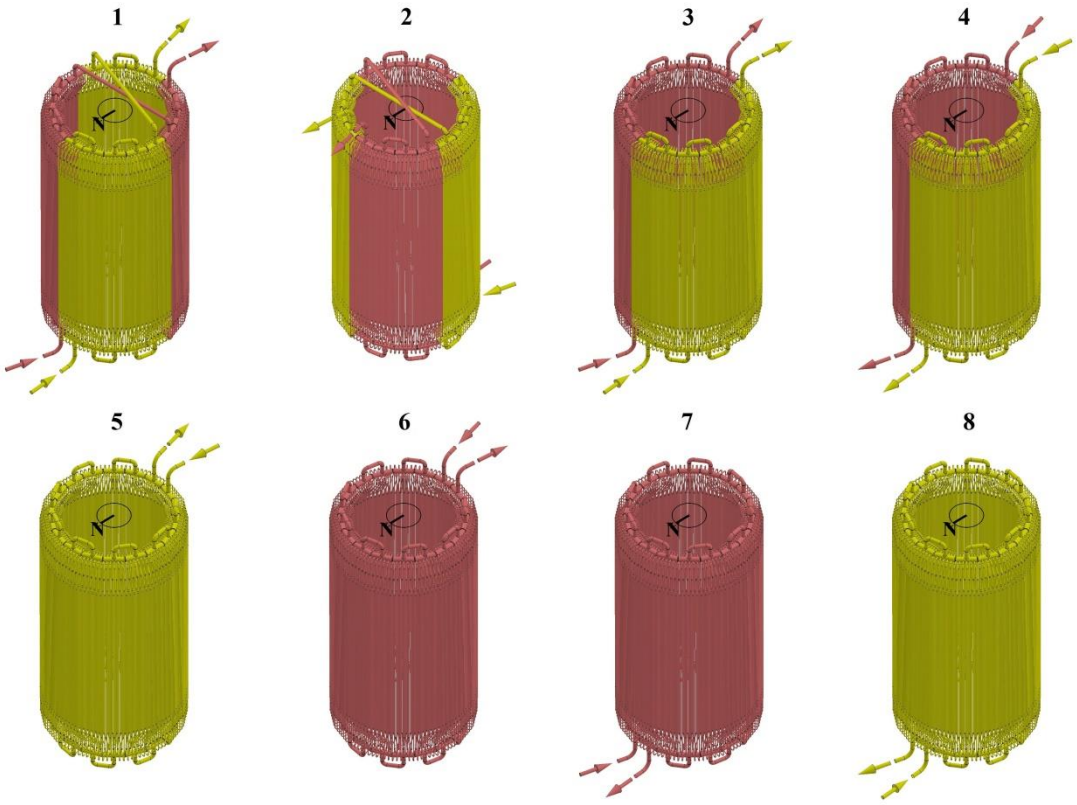

Figure 1. Receiver scheme for the eight flow pattern configurations proposed.

Figure 2 shows the top view of a receiver formed by 18 panels divided in two flow paths without crosses. The panels have been named from north to south and considering west and east orientation; this notation has been used from now on along the study.

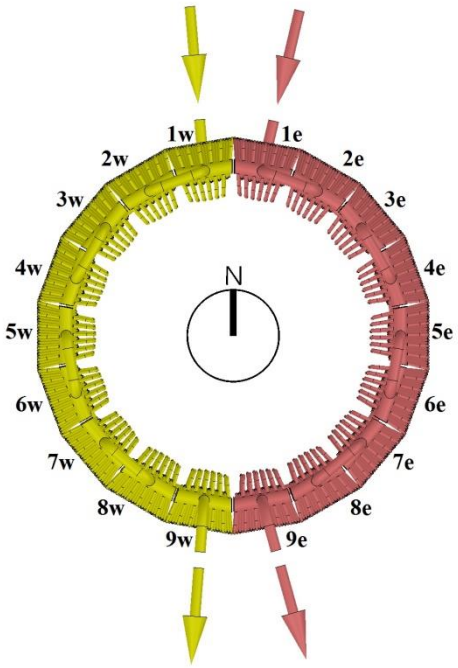

Figure 2. Top view of a receiver scheme with panel numeration.

Wagner (Wagner, 2008) studied the different flow configurations based on the thermal losses of the receiver. He showed that configurations with only one flow path have higher pressure drop and increase the parasitic consumption. Hence to reach higher thermal efficiency of the receiver the panels must be arranged in two parallel paths (configurations 1 to 4). Of the four multiple flow patterns analysed the most efficient configurations, in the northern hemisphere, are south-to-north flow with none or one crossover (configurations 4 and 2, respectively). This is so because the solar peak flux is maximum in the north side of the receiver. Wagner claimed that if the cold HTF enters by the northern panels its temperature increases rapidly, and the hot HTF that travels to the west-south/east-south panels contributes to elevate the tube wall temperature of the receiver, increasing the heat losses by radiation and convection. Wagner

also claimed that thermal stress is highest in the panels where the flux on the receiver surface is highest regardless of fluid temperature. At solar noon the incident flux in the last panels of the south-to-north flow is maximum and the salt temperature is elevated causing problems of thermal stress.

The solar-noon of the spring equinox is usually used as design point of SPT (Kistler, 1986; Winter et al., 1991). (Collado, 2009) studied the heliostat field efficiency for different layouts; he showed that at the solar-noon the efficiency of a circular heliostat field is symmetric with respect to the north-south axis. In addition, Augsburger et al. (Augsburger and Favrat, 2013) proved that the 12 solar time presents a symmetric flux radiation map on the receiver with respect to the north-south axis for a heliostat field like Gemasolar, locating the peak flux in the northern panels of the receiver, in the northern hemisphere. Hence, for a two flow path receiver configuration the solar flux absorbed in solar-noon by both flow paths is the same, and the crossover configuration is in the background. Nevertheless, in the northern hemisphere during the sunrise and sunset the maximum solar radiation is displaced to the western and eastern panels of the receiver, respectively; producing an energy asymmetry between both flow paths. At these moments the crossovers are particularly important.

Kolb et al. (Kolb et al., 2011) predicted an availability of 90% for commercial plants in 2020, however until the moment only 85% has been achieved (Baharoon et al., 2015). They identified the receiver system as one the most important causes of SPT unavailability. In this paper the optimal flow configuration has been analysed taking into account thermal, mechanical, and hydrodynamic factors to increase the receiver availability during a whole year, as well as to increase the overall efficiency of the SPT.

First of all, the critical operational limits which assure the receiver service have been established. The operation limits of the receiver are the minimum mass flow rate, which determines the start-up and shut-down of the receiver; the maximum film temperature to

avoid tube material corrosion and molten salt decomposition; and maximum thermal stresses to avoid fatigue and cracking. Once the operational limits have been defined, the most adequate receiver flow configuration of the eight proposed can be determined for the design-point. In that step, an optimum receiver design formed by tubes of 4.22 cm of diameter arranged in 18 panels, and previously obtained by Rodríguez-Sánchez et al. (Rodríguez-Sánchez et al., 2014b) has been used as particular case of study.

Secondly, the possible hours of operation during a whole year for the selected configuration have been analysed, and the relation between the direct normal irradiation (DNI) and the elevation angle of the sun (by means of the flux density on the receiver) that indicates the hour at which the receiver could start/stop to operate has been calculated. At the same time it is possible to determine the critical hours of operation of a receiver:

- First hours in the morning and last hours in the afternoon. During these hours the most critical parameters are the flux asymmetry between flow paths, and the internal convective heat transfer coefficient (defined by the molten salt velocity).
- Hours in which the flux peak is high but the flux is non-symmetrically distributed between paths. In these hours the most critical factors are the film temperature and the thermal stresses.

Finally, an example of each critical hour has been analysed in order to find the crossover position that optimizes the whole range of operation of the receiver and increases the receiver availability, increasing also the annual power generated for the SPT and its global efficiency.

2. Receiver and field description

Rodriguez-Sanchez et al. (Rodríguez-Sánchez et al., 2014b) studied the optimum receiver design based on thermal, mechanical, and hydrodynamic analysis for a SPT of 120 MWt with molten salt as HTF, located in Seville (Spain). The design point of that receiver was the solar-noon of the spring equinox. The receiver consists of 10 m of height and 8.4 m of diameter of

Incoloy 800H, formed by 18 panels of 32 tubes each. The external tube diameter is 4.22 cm and the internal 3.89 cm. The receiver has a total weight of 10 tons of stainless steel. In addition, the receiver is divided in two flow paths from north to south, and at nominal conditions it fulfils the maximum film temperature for Incoloy 800H. However, in the previous work neither the detailed analysis of the flow pattern nor the number of hours in which the receiver could work under safety operation were considered.

In this paper the flow pattern configuration of the receiver has been optimized. To calculate the flux density incident on the receiver, the computational optical model developed by Sanchez-Gonzalez and Santana (A Sánchez-González and Santana, 2015) based on the analytic function at the image plane (Collado et al., 1986) has been employed. The heliostat field has been configured as Gemasolar, whose 2650 heliostat coordinates were retrieved from a scaled aerial photograph. Square heliostat mirrors are 10.95 m side with 0.88 reflectivity and 0.95 cleanliness. Sun, slope and tracking errors are 2.51, 2.6 and 2.1 mrad, respectively.

In the absence of specific aim-point information, a previously reported multi-aiming strategy (A Sánchez-González and Santana, 2015) has been applied in the computational model. The aiming factor has been adjusted for the different days and hours, in order to reduce the tube wall temperature as much as possible with an acceptable level of receiver efficiency. In addition, the number of heliostats aiming at the receiver has been reduced in days of high insolation.

3. Operation limits

The operational strategy in SPT is to drain the molten-salt each night and turn-off the heat trace in order to reduce the parasitic power consumption of the plant (Pacheco et al., 1995). In the early morning the panels of the receiver are preheated with the heliostats before they are filled with molten salt. Vant-Hull (Vant-Hull, 2002) showed that this preheating process is typically accomplished in 15 minutes using a maximum flux density of 36 kW/m^2.

Consequently, the external receivers could start-up as early as the blocking and shadowing factors (caused by low elevation angles of the sun) allow it.

After sunrise, the receiver starts-up when the heat absorbed by the receiver is enough to assure the proper operation of the receiver. There are authors that claims that the receiver starts to operate at 10° of sun elevation angle (Falcone, 1986) , while others say that the limiting elevation angle is 15° (Collado and Guallar, 2013). Delay the start-up to a sun elevation angle of 10° or 15° represents a loss of 0.7 or 1hours of possible operation per day, respectively.

In this research, it has been studied the hour at which the receiver could start to operate, as long as the sky is free of cloud and haze, and taking into account that there are certain thermal, mechanic and hydrodynamic limits that the receiver must not overpass. The operational limits has been calculated with the receiver thermal model developed by Rodriguez-Sanchez et al. (Rodríguez-Sánchez et al., 2014b). It has been imposed that in both paths the salt enters at 290 °C and exits at 565 °C, at the expense of the mass flow rate variation.

To carry out the analysis only an averaged representative day per month has been studied since the solar angle variation between two consecutive days is negligible, and the hourly DNI of a whole year is impossible to predict. The hourly statistics for direct normal solar radiation and the average hourly statistics for dry bulb temperature in Seville have been obtained from IWEC data (US Department of Energy, 2013). Each of them corresponds to the most representative month of a sample of years from 1982 to 1993.

3.1. Minimum mass flow rate

The operational range of the bulk temperature of the salt is limited by its freezing point and by its decomposition rate. The typical work range of a molten salt receiver is from 290 °C at the

inlet to 565 °C at the outlet. Hence, it is possible to calculate the nominal mass flow of the receiver for a given receiver power. The nominal mass flow for a receiver of 120 MW_t is 290kg/s .Where Cp corresponds to the average specific heat of the salt at mean work temperature, 1516.5 J/kgK (Zavoico, 2001). In this study the minimum allowable mass flow rate has been chosen paying attention to the feed pumps operation range but also to the conditions of turbulent flow regime required.

Authors as Kolb (Kolb, 2011) fixed the minimum operation range of the molten salt receiver in 10% of the nominal mass flow rate. Whereas, Falcone (Falcone, 1986) planned the control system of Solar 100 to maintain the mass flow rate of each circuit at a minimum of 20% of the nominal case under low power conditions. The feed pump system of a SPT is usually compounded by one or more long-shafted pumps working in parallel. In the case of Solar Two, the circulation pump is a single vertical pump of 14 m of shaft length (Zavoico, 2001). In the planned plant Solar 100, the design counts three half-capacity receiver feed pumps, each of them has a 50% capacity of the nominal flow, keeping one pump in reserve. In this research it has been considered different pump systems configurations with variable minimum allowable mass flow rate.

The dependence of the heat transfer coefficient on the velocity and therefore on the mass flow rate must be taken into account since forced convective heat transfer is influenced by the flow regime (Pugh and Garvey, 1993). The flow regime depends on the DNI and the flux density on the receiver. To obtain a homogeneous bulk temperature in the tubes of a solar receiver the flow must be under turbulent regime.

The Nusselt number (Nu) for laminar flow is very low (Nu_l = 4.36), and hence a laminar flow causes failure in the receiver by corrosion and thermal stress due to the lack of cooling of the tube walls. The accurate prediction of Nusselt number in the transition flow region is difficult, Cheesewright et al. (Cheesewright et al., 2001) recommended a linear interpolation of the

values of Nusselt number for laminar and turbulent (Nu_t) flow over a transition region (see Equations 1 and 2). The worst scenario for the Reynolds number are the inlet of the cold salt, if in the first panel has high solar flux, the molten salt under the transition region could damage the receiver by tube overheating. On the other hand, if this panel has low solar flux the salt could freeze inside the tubes. To avoid damages in the receiver it has been imposed the turbulent region as the lower operational limit, Re >4000. The turbulent Nusselt number can be calculated by the Petukhov correlation (Petukhov, 1970) (see Equations 3 and 4).

$$Nu = \varepsilon Nu_l + (1-\varepsilon) Nu_t \quad \text{(Eq. 1)}$$

$$\varepsilon = 1.33 \frac{\mathrm{Re}}{6000} \quad \text{(Eq. 2)}$$

$$Nu_t = \frac{f/2\,\mathrm{Re}\,\mathrm{Pr}}{1.07 + 12.7\sqrt{f/2}\left(\mathrm{Pr}^{2/3}-1\right)} \quad \text{(Eq. 3)}$$

$$f = \frac{1}{4\left(1.82\log \mathrm{Re} - 1.64\right)^2} \quad \text{(Eq. 4)}$$

Note that the limit of the pure turbulent limit found in the bibliography for other authors is at Reynold 10,000 (Aicher and Martin, 1997). It makes that when the receiver start-up at first hours in the morning could operates in mixed turbulent flow, it is not the most favourable operation condition for the receiver but the convective coefficient at that velocity is enough to avoid overheating in the tubes. It has been taken into account that the convective coefficient varies a 10% with respect the pure turbulent regime, although it is compensate between down-flow and up-flow panels.

Using the geometry defined in Rodríguez-Sánchez et al. it is possible to calculate the thermal and mechanical behavior of the receiver using a 2D thermal model previously depicted by

(Rodríguez-Sánchez et al., 2014b). This receiver model is a 2D simplified thermal model of the receiver that considers temperature variations in both axial and circumferential directions.

Known the solar flux density, obtained with the heliostat model of (Alberto Sánchez-González and Santana, 2015), the heat flux absorbed by the tubes have been calculated by means of the Net Radiation Method (Modest, 2003), the cross-string method view-factors, and the Siebers and Kraabel correlation for the external convective losses (Siebers and Kraabel, 1984). Fixed the outlet temperature of the salt and applying an energy balance to the tubes in which the Petukhov correlation for internal convection (Petukhov, 1970) it is used, it is possible to determine the mass flow rate in the receiver, the bulk temperature of the salt, and the tube surface temperature.

Then, for the optimal design the velocity limit for turbulent regime (Re =4000) in the receiver tubes is $v_{\min}$ = 0.19 m/s (Equation 5). It has been assumed that the salt flow is regulated by control valves to maintain 565 °C as outlet temperature in both flow paths, and then the mass flow rate of each path is only a function of the total solar flux received. That supposes a minimum allowable mass flow rate ($\dot{m}_{\min}$) of 13.77 kg/s when only one flow path is implemented or 27.37 kg/s when the receiver is formed by two flow paths (Equation 6). Therefore, if the pump system limit is lower than 5% or 10% of the nominal mass flow rate, for one and two flow path configurations respectively, the turbulent regime is the most restrictive criteria.

$$v_{\min} = \frac{\mathrm{Re}_{\min}\,\mu}{\rho dt_{\mathrm{int}}} \qquad \text{(Eq 5)}$$

$$\dot{m}_{\min} = v_{\min}\rho\frac{\pi}{4}dt_{\mathrm{int}}{}^{2}N_{tubes}N_{fp} \qquad \text{(Eq 6)}$$

In Equations 5 to 6 μ corresponds to the dynamic viscosity of the salt at the inlet temperatures of the salt (0.0035 Pa/s), ρ represents the density of the salt at 290 °C (1905.7

kg/m3), N_{tubes} represents the number of tubes per panel, and N_{fp} is the number of flow paths in the receiver.

Note that the limit for turbulent regime calculated is valid for any tube diameter configuration if the number of receiver panels is constant. When the diameter of tubes decreases, the number of tubes per panel increases, and the Reynolds number remains almost constant. For example, using tube diameters of 2.5 cm the Reynolds number increases only 2%, nevertheless the pressure drop increases 67.5%. Therefore, to reduce the tube diameter does not assure turbulent regime during the start-up and shut-down. However, modifying the number of panels of the receiver the Reynolds number varies as the ratio of number of tubes per panel and the pressure drop increment is the Reynold ratio raised to the second power. Increasing the number of panels to 20 the Reynold number increases 12.5% and the problems in the start-up and shut-down disappear, although other properties of the receiver get worse (Rodríguez-Sánchez et al., 2014b).

The minimum incident power on the receiver to start to operate can be calculated using Equation 7, where the power absorbed by the salt is calculated using the specific heat of the salt at the inlet of the receiver (Cp_{in} = 1493 J/kgK), $\sum C$ corresponds to the sum of the solar flux intercepted by the receiver surface. S is the surface area of each cell in the receiver defined in the optical model, and η_{rec} represents the receiver efficiency, which is calculated with the receiver thermal model that strongly depends on the incident power flux on the receiver and its distribution, the ambient temperature, and the flow pattern.

$$\dot{Q}_{rec} = \frac{\dot{Q}_{salt}}{\eta_{rec}} = \sum C \cdot DNI \cdot S \cdot N_{tubes} \qquad \text{(Eq 7)}$$

3.2. Maximum film temperature and thermal stress

Salt at temperature above the stability limit is in contact with common materials such as stainless steels and nickel alloys, there is an extensive corrosion with the release of nitrogen oxides due to the reaction between the solar salt and chromium to form chromates (Nissen and Meeker, 1983).In addition, up to 620 °C there is a thermal decomposition of the solar salt that increases the tube corrosion (Abe et al., 1984). The maximum allowable film temperature is defined as the parameter that drastically increases the corrosion rate. Slusser et al. (Slusser et al., 1985) performed corrosion tests of several metals in molten nitrate-nitrite salts for a range of temperatures between 570 and 705 °C. In their tests nickel based alloys, such incoloy 800H, were resistant to corrosion up to 650 °C.

In addition, the admissible thermal stress in the tubes of the receiver is delimited by ASME nuclear code: ASME Boiler and Pressure Vessel Code, Section III, Division 1-subsection NH: Rules for construction of nuclear facility components (American Society of Mechanical Engineers (ASME), 2011), which is more conservative and specific for the stress and fatigue calculations than those used for boilers. The maximum thermal stress allowed by this code is one third of the ultimate tensile strength.

4. Receiver flow path selection

In this section the optimal receiver flow pattern configuration for the nominal conditions of the design point has been obtained based on thermos-mechanical and hydrodynamic limitations. The cases studied are the eight flow path configurations proposed by Wagner (Wagner, 2008) shown in Figure 1.

Figure 3 shows the thermal efficiency of the receiver, the total pressure drop, the maximum film temperature and the maximum thermal stress of each one of the eight proposed configurations for the solar noon of the spring equinox. For all the cases the same aiming strategy has been employed: one aiming point to the centre of the receiver with an opening radius corresponding to a normal of standard deviation 2.5, see (Alberto Sánchez-González and

Santana, 2015). It can be seen that the maximum thermal efficiency is obtained for configurations 2 and 4, two paths with south to north flow, as Wagner predicted. However, the receiver efficiency is 77.2% instead of Wagner's 95%. This difference is caused by taking in consideration circumferential variations of the tube wall temperature (Rodríguez-Sánchez et al., 2014a).

For configurations 2 and 4 the tube film temperature and the thermal stresses are over the allowable value, producing corrosion and fatigue in the tubes, therefore it is not secure to use them. As Wagner claimed, configurations 5 to 8 (one flow path configurations), are discarded due to the elevated pressure drop that produces a high power consumption of the feed pumps. This increment of the parasitic consumption of the SPT has to be analysed in detail for configurations 5 and 6, which reach safe values of film temperature and thermal stresses. Configurations 1 and 3 (with two flow paths north-to-south configurations), fulfil film temperature, thermal stress and pressure drop restrictions necessary to assure the receiver lifetime. However, these configurations have the worst receiver efficiency, even though it is only around 1 % lower than configurations 2 and 4.

Therefore, it can be seen that the worse configurations- regarding film temperature and thermal efficiency- are those in which the outlet is at the northern panels. From the four configurations with the outlet at the southern face, the most favourable are those with two flow paths. Such configurations mean 0.5 % less efficiency than one path, but this reduction is lower than the reduction in the SPT global efficiency caused by an increment of 5 bars in the pressure drop. Consequently, configurations 1 and 3 have the most adequate flow pattern to be used for the proposed operational conditions.

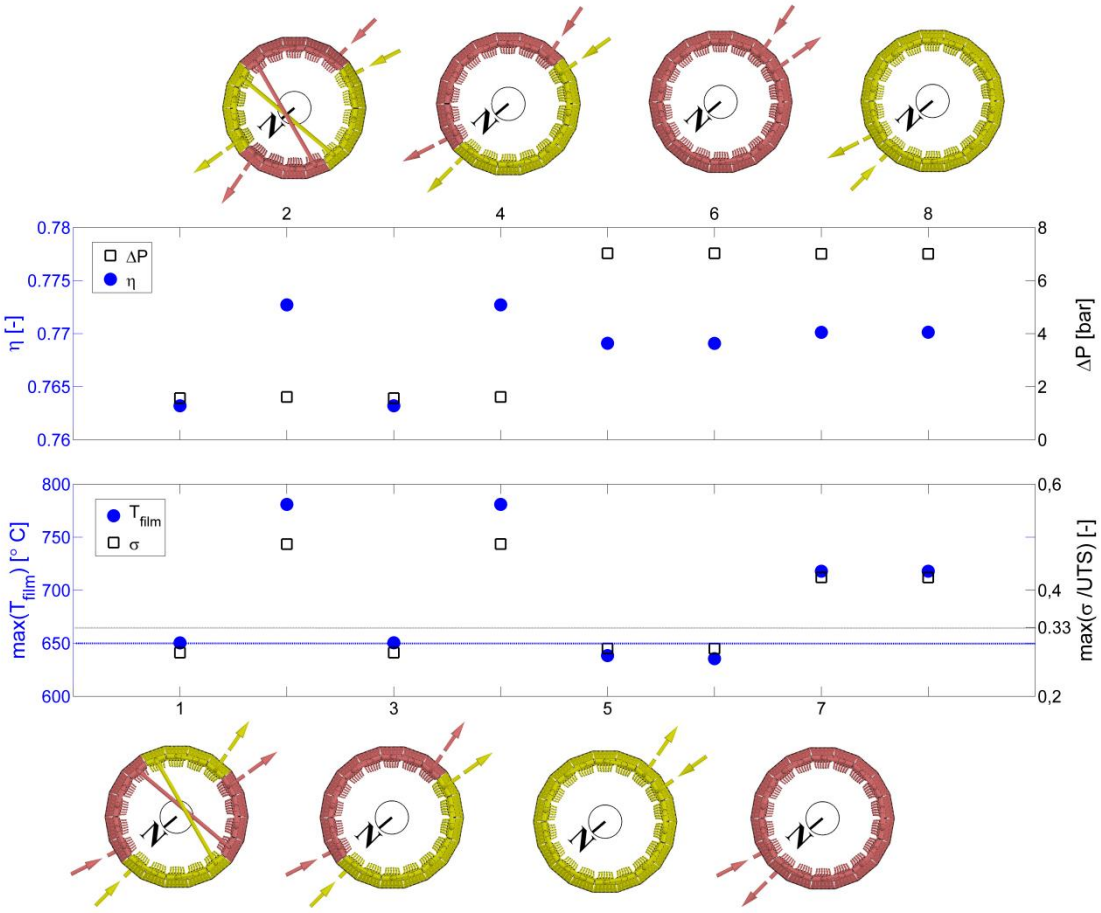

Figure 3: Receiver thermal efficiency, pressure drop, maximum film temperature and maximum thermal stress of the eight proposed flow path configurations.

At solar-noon the behaviour of configuration 1 and 3 are identical, however at hours with non-symmetric solar flux the behaviour of these configurations is different. It has been studied which of them is the most appropriate configuration for the whole annual range of the receiver operation. In addition, for configuration 1 the position in the crossover has been modified in order to increase the annual availability of the receiver.

5. Results

Once the optimal configuration is chosen, the possible hours of operation of a receiver with two flow paths north-to south during a whole year have been determined. There are certain

hours in which the correct operation of the receiver cannot be assured, these hours have been identified and carefully analysed.

The simplest flow pattern is the absence of crossovers between the receiver flow paths. However, far from the solar-noon the solar flux intercepted is asymmetric between both flow paths. For the critical hours of operation, it has been analysed if the asymmetric solar flux between flow paths causes damages in the receiver, and if crossover between flow paths must be implemented. Or on the contrary if the solar flux asymmetry could be supported, and it is preferable not to cross the flow. In addition, modifications in the crossover position have been tested in order to increase the availability and annual efficiency of the receiver. For all the analysed cases, it has been assumed that only flow limitation that must be taken into account is the turbulent flow regime, $\mathrm{Re} \geq 4000$.

5.1. Possible hours of operation along a year

The hours of the year, in which the solar radiation is not enough to start-up the receiver, although the sun is above the horizon, have been determined using the DNI, the ambient temperature, and the solar flux concentration ratio. The flux density has been calculated using the solar field model proposed by (A Sánchez-González and Santana, 2015). It must be taken into account that the DNI, at a given instant of time, represents the typical value of a representative day of a month, but it can vary along the month, or include haze and cloudy days in which the receiver cannot work (see Figure 4.a).

Using the receiver modelling of Rodriguez-Sanchez et al. (Rodríguez-Sánchez et al., 2014b) without the implementation of crossovers, the thermal efficiency of the receiver and the power absorbed by the salt have been calculated. At first hours of operation the receiver has efficiencies near to 50%, but it grows quickly and when, the radiation is close to the nominal value, the efficiency of the receiver reaches 77%, as can be observed in Figure 4.b.

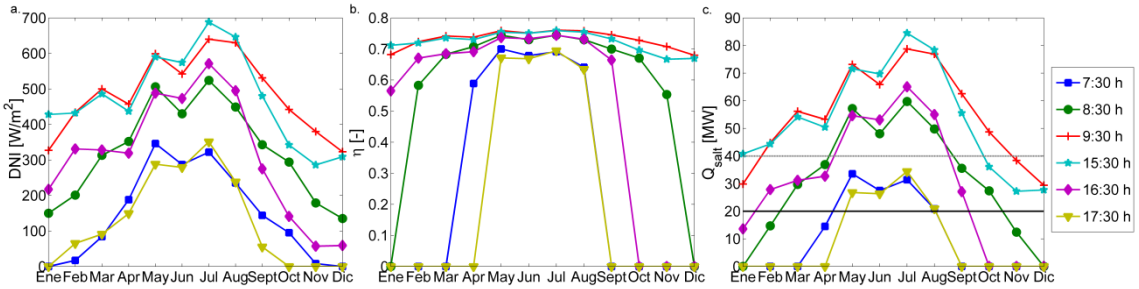

Figure 4. a) Average hourly statistics direct normal solar radiation. b) Average thermal efficiency of the receiver. c) Average heat absorbed by the salt. All data corresponds to Seville (Spain) for a representative year.

Figure 4.c represents the total power absorbed by the salt at each hour. The horizontal solid black line delimits the turbulent flow regime (Q_{salt} = 19.98 MW). When the power is under that value the flow is under transient regime. At these hours the receiver integrity could be compromised, and therefore it has been assumed that the receiver is not working. In addition, the grey dotted line shows the limit of operation of a SPT when the pump system is unable to operate at mass flow rate lower than 20% of the nominal flow, as happen in Solar 100 (Falcone, 1986). In this case, the hours of operation of the receiver decrease 660 h per year respect to the turbulent regime limit. Then, a proper design of the pump system is a key to keep at maximum the availability of SPT. In Figure 4.c it can be also observed that due to the difference in the flux density between summer and winter, in winter months the minimum DNI to start to operate the receiver is 170 W/m^2, while in summer is enough a solar direct irradiance of 100 W/m^2.

Figure 5 depicts the average hours of sun of each month, the hours in which the radiation flux is enough to heat the salt, and the hours at which the receiver can operate at turbulent regime. It can be observed that the receiver starts-up at least one hour after the sunrise (~15° of solar elevation), time enough to preheat the tube walls; while the shut-down are at least one hour before sunset, reducing the stress cycles of cooling. In addition, depending on the season the start-up varies from 7:00 h to 9:00 h and the shut-down from 15:00 h to 17:00 h, all

respect to solar time, modifying the panel which receives the peak flux in the start-up and shut-down along the year.

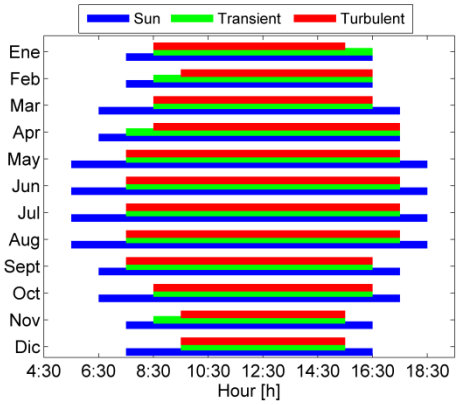

Figure 5: Average hours of sun per month and hours of possible operation of the receiver.

5.2. Critical hours of operation

The optimal flow pattern configuration must fulfil the operational limits of the receiver for the whole operational range. In addition, it has to maximise the annual availability and efficiency of the SPT.

Therefore, it is necessary to analyse the first hours in the morning and the last hours in the afternoon, in which problems associated with salt velocity can appear. During the sunrise and sunset the receiver operation restrictions are the limits of the feed pumps and the turbulent regime. In addition, the periods of high peak flux with not symmetric distribution with respect to the north- south axis must be studied to avoid excessive film temperature and thermal stresses. In case of big feed pump systems the start-up and shut-down analysis is not crucial, because there is enough flux concentration. Nevertheless, the hours with high solar irradiation but non-symmetrically distributed continue being critical.

Figure 6 shows the solar flux distribution on the receiver for the design point and for three examples of critical hours: first hour in the morning, last hour in the afternoon, and high peak flux non-symmetrically distributed between paths. Where *x* axis corresponds to the

circumferential perimeter of the receiver counter-clockwise from the south, as can be seen in the panel numeration, and *y* axis represents the receiver height.

In spring equinox at solar-noon the solar flux is totally symmetric with respect both flow paths (see Figure 6.a). Coming back to Figure 4.c the most limiting hours analysed for turbulent flow 7:00 h and 17:00 h of August, Figure 6.b and Figure 6.c respectively. Both hours are mirrored images with respect to the solar-noon. Then, they receive the same total solar flux, but it is distributed symmetrically with respect to the north-south axis. Consequently, the results of the east side for 7:00 h are equivalent to the results of the west side for 17:00 h and vice versa. As first hours in the morning and last hours in the afternoon are symmetrical, only one hour has been studied in detail choosing 7:00 h as reference. Furthermore, it can be seen that they have very low flux concentration compared to the design point. Finally, Figure 6.d depicts May at 9:00 h. It is a clear example of high peak flux non-symmetrically distributed between paths. At this hour the peak flux is more centred to north than the case of august at 7:00/17:00 h, but less than the spring equinox at 12:00 h.

In Figure 6 the maximum solar flux ranges go from 0.24 MW/m^2 at first/last hours of August, to 0.65 MW/m^2 at 9:00 h of May, and to 0.8 MW/m^2 at the solar noon of the spring equinox.

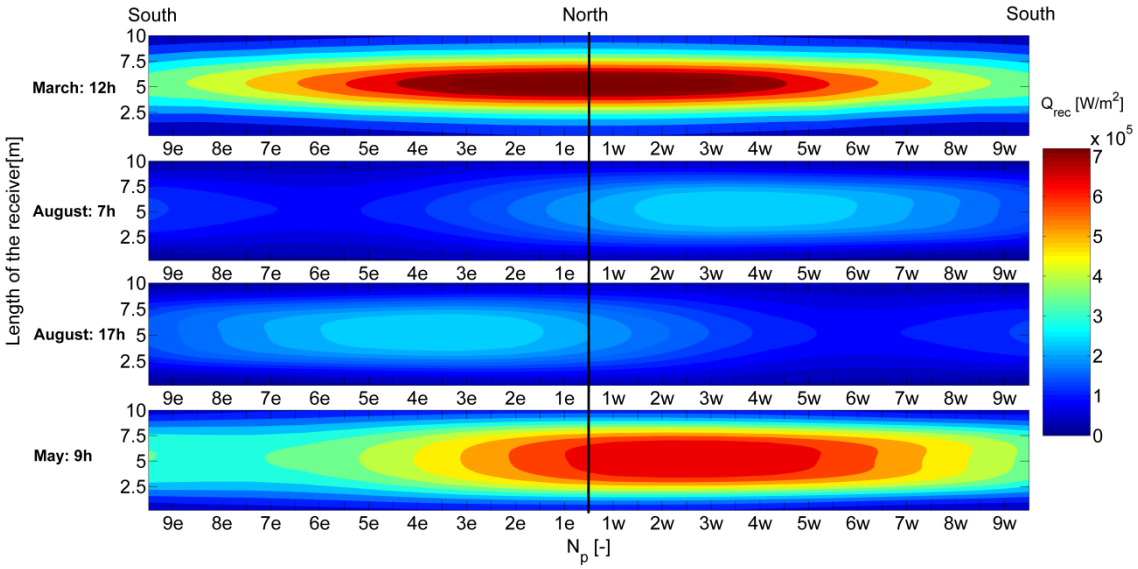

Figure 6: Radiation map distribution on the receiver. From top to bottom: Design point (spring equinox at 12:00 h); Start-up (7:00 h of August); Shut-down (17:00 h August); and Non-symmetric high peak flux (9:00 h of May).

5.3. Optimal crossover position

The asymmetric solar flux between flow paths can reduce the receiver operational hours when the solar flux is non-homogeneously distributed between paths and the solar flux is low. Under these conditions, the convective heat transfer coefficient in one of the paths might not able to refrigerate the tube wall. Implementing crossovers the energy absorbed by both paths could be equalised. However, reaching the same quantity of flux could be undesirable if the solar flux distribution with the crossovers has the peak at the outlet of the receiver. High solar flux in panels in which the salt is too hot could increase the tube wall temperature and the thermal stresses. Then, the film temperature of the path could overpass the limit established by the receiver material accelerating the corrosion process and diminishing the lifetime of the receiver.

In this section has been chosen which of the two selected flow patterns it is the most adequate configuration for a whole year operation range. The behaviour of receivers have been analysed for the critical hours of operation. Remember that the selected receivers are composed by two flow paths north-to-south with none (configuration 3 of Figure 3) or one crossover in the middle of the panel (configuration 1 of Figure 3). In the case of configuration 1 different crossover positions have been implemented in order to find the most adequate flow configuration.

The selection of the best receiver flow path configuration has been done following the procedure showed in Figure 7. It starts with a known heliostat field, receiver geometry, and location. Firstly, different path crossover configurations for start-up and shut-down are analysed in order to find the optimal configuration that increase the receiver availability. After

that, it is proved if the optimal path configuration for start-up and shut-down is valid for those hours of high peak flux but non-symmetric flux distribution between paths.

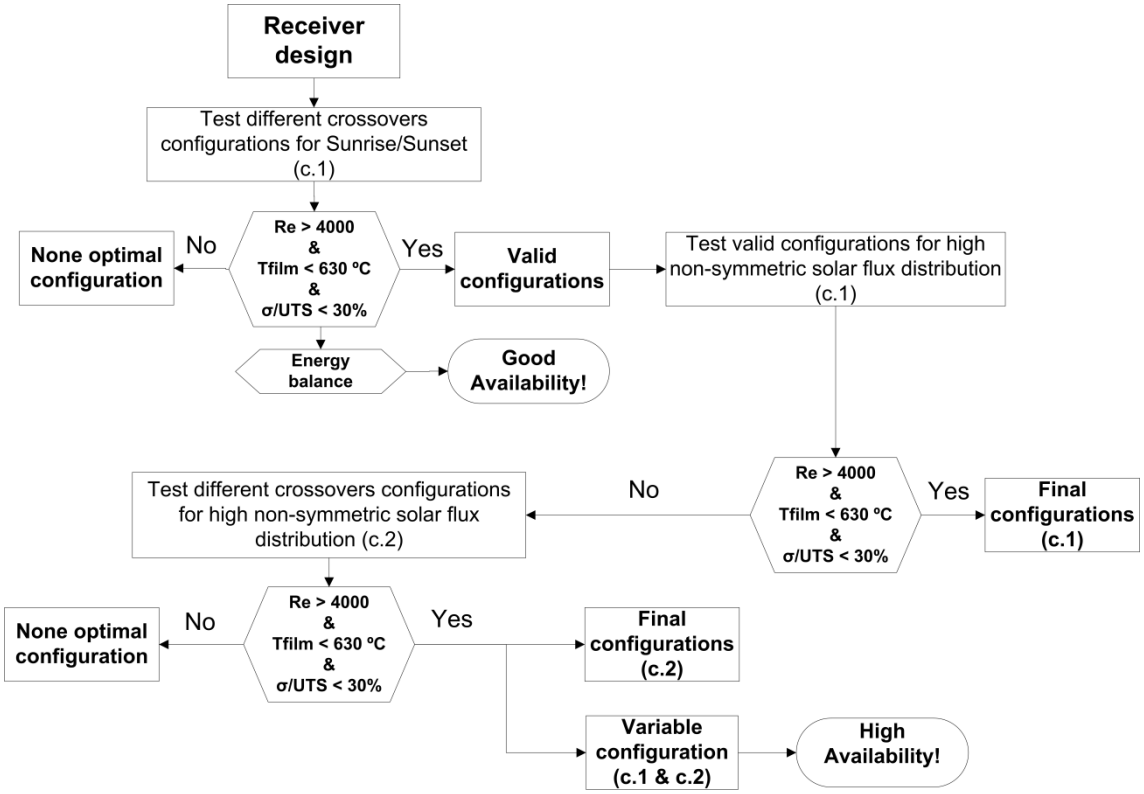

Figure 7. Scheme procedure to optimize the flow pattern configuration of a solar external receiver.

5.3.1. Start-up and shut down (August at 7:00 h)

Figure 8 shows the variation of the solar radiation distribution over the two flow paths of the receiver when one crossover is applied at 7:00 solar hour of August (configuration 1). Vertical axis represents the height of the receiver, and horizontal axis the panel number of each flow path, from 1 to 9 east and west. There are 8 possible combinations of crossovers, but for clarity only have been plotted the configurations with crosses at the even panels of each path. In addition, the flow pattern without crosses (configuration 3) has been represented to observe the differences. It can be seen that in absence of crossovers the maximum heat flux is not in the western panels, else it is slightly displaced to the north.

When there is a cross in the receiver the flow path goes from north to south changing the side from west to east and vice versa; it means that if the radiation map it is not symmetric, as happens at 7:00 solar time, the incident flux could have step variations. For example, for a crossover in the fourth panel the west flow path starts in the first panel sited in the north of the receiver, it continues by the west panels until the west fourth panel, and in the fifth panel the flow path is crossed and the radiation flux of the fifth panel corresponds to the east fifth panel instead of the west fifth panel.

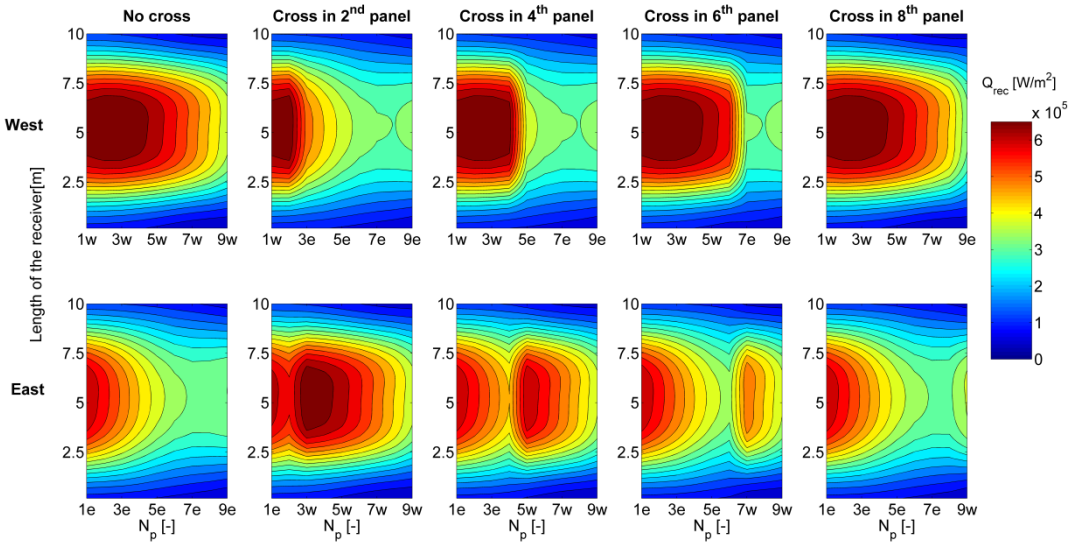

Figure 8: Radiation map distribution on the receiver at 7:00 h of August with none or one crossover between flow paths.

In the ideal configuration both flow paths must absorb the same energy, and the maximum solar radiation has to be in the first panels of the receiver, what reduces the thermal stresses and the tube wall temperature. The total solar flux received by both flow paths is equal when the cross is implemented in the 4th panel (see Figure 9). However, this configuration is not the most adequate because the maximum solar radiation is close to the western and eastern panels, affecting to the film temperature (see Figure 6). To obtain the ideal configuration is not possible using only one crossover in the receiver, but varying the crossover position the receiver behaviour can be improved.

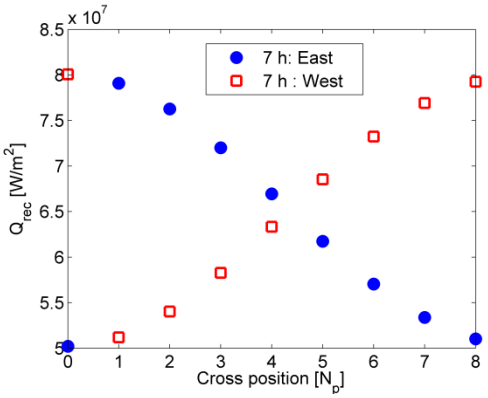

Figure 9: Solar flux received by each flow path, for one crossover in different positions at 7:00 h of August.

Figure 10 represents mechanic, thermal and hydrodynamic variables when one crossover is applied to the receiver flow paths. The position 0 corresponds to the nominal case in which none crossovers in the receiver is installed, the followings data from 1 to 8 correspond to the variation of the crossover position, from the outlet of the first panel to the outlet of the 8 panel of each path. For the different crossover positions the efficiency of the receiver is almost constant and equal to 64.2%, because the receiver is not working in its nominal conditions.

Figure 10.a portrays the minimum salt velocity in the tubes; it takes place at the inlet of the receiver, when the salt is cold and the density reaches the highest value. It is possible to observe that without crossovers the salt velocity in the east side is lower than the turbulent regime limit. Similar results are obtained crossing in the first or last panel of the path (asymmetric solar flux between paths). An allowable salt velocity can be achieved crossing in any positions from the 2nd panel to the 7th panel. However, apply the cross at the ending of the 4th or 5th panel are the best configurations.

The total pressure drop, showed in Figure 10.b, is lower than the pressure drop limit imposed by the power consumption of the pump system. Hence, pressure drop does not present any problem during the receiver start-up. It can be seen that velocity and pressure drop only

depend on the total flux that reach each path but not on the solar flux distribution. However, thermal stresses and film temperature depend on both variables.

The maximum film temperature of the receiver increases drastically with the position of the flow path crossover (see Figure 10.c). However, it never overpasses the allowable limit of the alloy 800H. To cross in the last panels is not adequate due to the peak solar flux is displaced to the last panels of the paths. Therefore, during the start-up of the receiver it is not recommendable to cross the flow paths after the middle of the path. In this specific day the best option to minimise the film temperature is to cross in the 3rd panel. The thermal stress is also below the allowable limit (see Figure 10.d); it reaches the minimum value crossing in the 3rd or 4th panel.

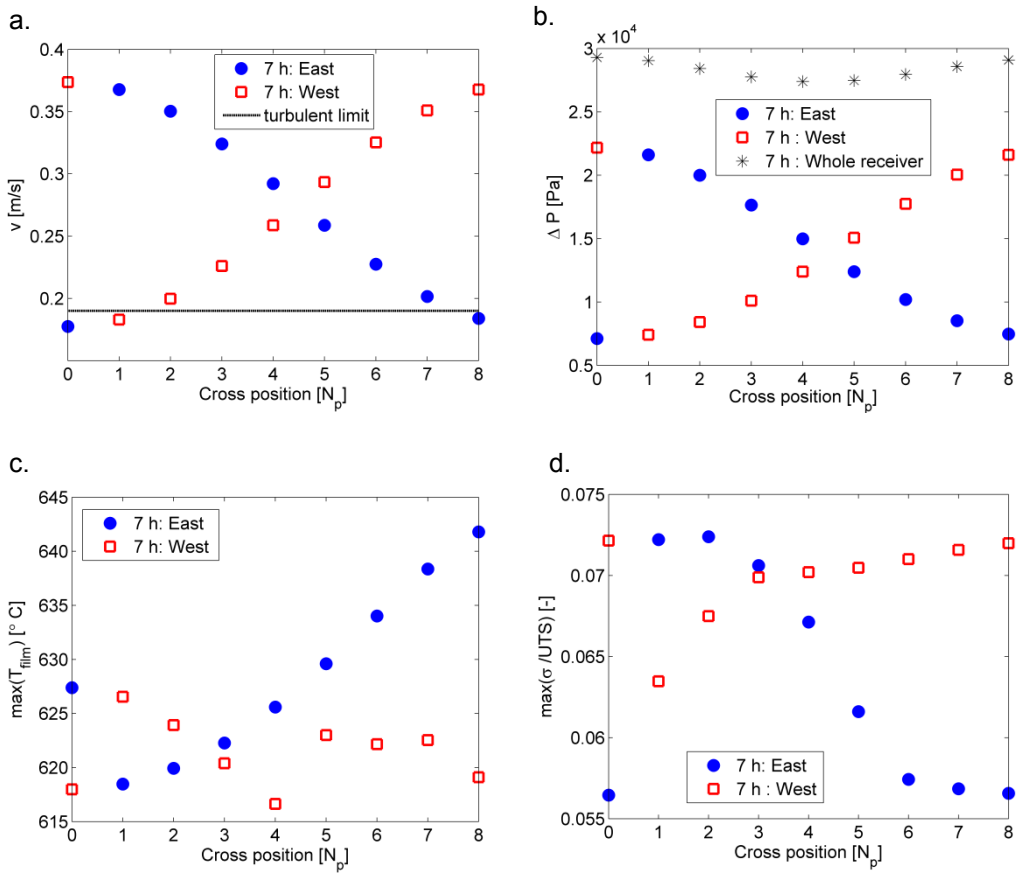

Figure 10. Implementation of one crossover in the receiver for 7:00 solar hour of August. a) Minimum salt velocity. b) Total pressure. c) Maximum film temperature. d) Maximum thermal stress.

Therefore, when the solar flux is low and not-symmetric between paths it is necessary to cross the flow path to equalise the flux between paths and increase the receiver availability. The maximum value of the solar flux is displaced several degrees to the north respect to the west side of the receiver, then it is necessary to cross before the middle of the path. The problem of cross in the first panels is that the flux that reaches to each path is not similar. In the light of the results, the best option seems to cross in the 4^{th} panel, which means equal heat flux in both paths and low film temperatures.

To complete the analysis, a configuration with two crossovers between paths has been implemented. High number of crossovers between the receiver flow paths homogenise the solar flux distribution between flow paths. However, it makes more complex the receiver operation, especially by the heat losses and pressure drop in the pipe that change the flow direction. In addition, the solar flux distribution continues being high in the last panels and the improvement obtained with respect one crossover are negligible. Then, one crossover is the preferable design in the sunrise and sunset, and implement higher number of crosses between paths has been rejected.

5.3.2. High peak flux non-symmetrically distributed (March at 9:00 h)

In this section, it has to be taken into account hours in which solar flux is high and not totally symmetric whit respect to north-south axis. In these moments the thermal stresses and the film temperature could cause damages in the receiver. To avoid efficiency reduction it has been tested if in hours in which the film temperature is close to the limit a modification of the heat flux distribution, by means of crossovers between paths, can reduce the temperature to allow the receiver to operate with high peak flux. It is the case of May at 9 h. In that moment the solar irradiation and the flux density are elevated, but the flux distribution is not symmetric between both flow paths (see Figure 6).

In this date the radiation map distribution is still non-symmetric with respect to the north-south axis. In this case the receiver is operating close to the nominal point, and the receiver efficiency is 75.9 %. Figure 11 shows that at 9:00 h of May the total solar flux is equal for both paths crossing in the 5th panel. However, it is not possible to cross the flow paths after the 2nd panel without increasing out of limits the film temperature and the thermal stresses on the receiver. Then, the solar flux in both flow paths must be different to avoid causing damages in the receiver.

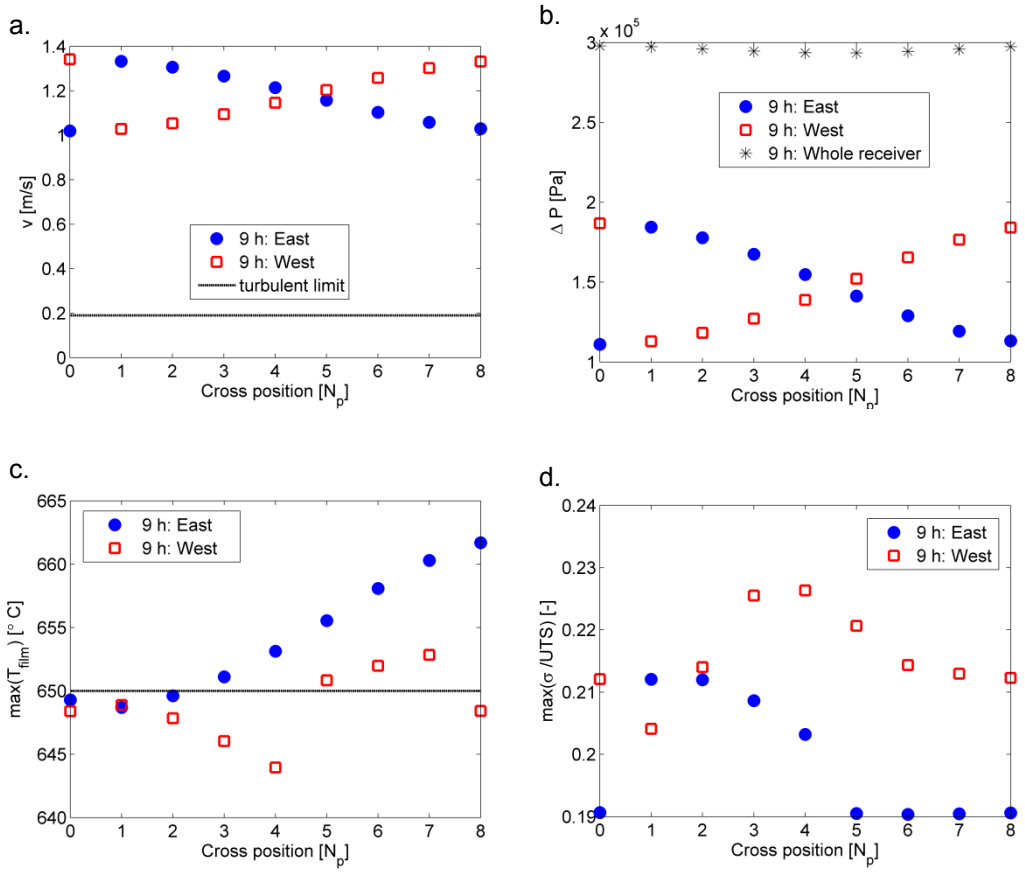

Figure 11. Implementation of one crossover in the receiver for May at 9:00 h solar time. a) Minimum salt velocity. b) Total pressure. c) Maximum film temperature. d) Maximum thermal stress.

Then, as the day passes the position of the optimal crossover approach the inlet of the flow path, and closer to the first panel the crossover has to be implemented. It made that the optimal crossover configuration for the start-up and shut-down is harmful for the receiver

when it received high peak flux non-symmetric distributed between paths. Then, in moments as 9:00 h of May, it is more important to get a well distributed solar flux than to have the same solar flux in both paths.

Therefore, the most adequate flow pattern is to employ a variable receiver crossover configuration. Implementing a crossover just before of the middle of the panel (in this case 4th panel) at first hours of the morning and last hours of the afternoon to increase the availability of the receiver. And remove the crossover when the receiver operates close to nominal conditions. If a variable configuration is not possible, it is recommendable not to implement any crossover in the receiver to assure the correct operation during hours of high efficiency, at the expenses of reducing the receiver availability. In nominal conditions the power obtained is higher than in the start-up and shut-down.

6. Conclusions

In this study different flow pattern configurations on molten-salt central receivers have been studied in order to assure the secure conditions of operation of the receiver in its whole range of work. Thermal, mechanical and hydrodynamic behaviour of the receiver at the design point have been analysed. It has been obtained that the best flow path configurations are those in which the flow exits by the south side of the receiver: it reduces the maximum film temperature and assures that the maximum solar flux is in the cooler side of the path, achieving a reduction of the thermal stress in the tubes. In addition, it is more desirable a configuration formed by two parallel flow paths to reduce the pressure drop for a given load. Then, the cold HTF must enter into the receiver at the panels that are exposed to higher solar flux and exits at the panels with lower solar radiation (from north to south in the northern hemisphere). The optimal flow path configuration can have none or one crossover between paths.

At the design point, receiver flow configurations with or without crossover have an identical behaviour. The critical hours of operation have been identified: the first hours in the morning, the last hours in the afternoon when the solar radiation is low and non-symmetric with respect north-south axis, and hours in which the peak flux is high but the radiation is not-symmetrically distributed between paths. The most important restriction to assure the correct operation of the receiver are the film temperature, the thermal stress, the pressure drop, the pump system and the convective heat transfer coefficient.

In order to absorb the same flux in both flow paths when the heat flux is not symmetric with respect to north-south axis, one crossover has been implemented in the receiver. The salt velocity and the pressure drop of both paths equalise when the solar flux in both paths is the same. However, the film temperature and thermal stresses depend on the solar flux received and its distribution. As sun moves to the midday the allowable positions of the crossover approach the inlet of the flow path, and it must be as close as possible to the first panel, although the solar flux sum is not always the same in both paths.

Although in this study the receiver geometry is fixed, it has been tested that the tube diameter does not modify the Reynolds number. Nevertheless, increasing the number of panels in the receiver also increases the Reynolds number, and the problems of transient regime in the sunrise and sunset disappear. However the pressure drop is strongly augmented.

To improve the heat flux distribution, receiving similar solar flux in both flow paths, during the start-up and shut-down of the receiver the best option is to implement one crossover in the 4^{th} panel of each flow path for a Gemasolar like receiver and heliostat field, in this way the mass flow per path is becomes equal, and there is no problems of transient regime flow. However, this configuration is not valid as the morning progresses. For these cases are recommended not to cross the flow paths. Consequently, the best receiver design will be that in which the flow path configuration can vary along the day; implementing one crossover before the middle

of the path during the sunrise and sunset, and removing the crossover when the solar irradiation is elevated. If this variation is not possible the most appropriate configuration is not to cross the flow paths. Since, it is more important a safe operation in the hours of maximum peak flux than during the starts-up and shuts-down.

Finally, in order to distribute more homogeneously the solar flux on the receiver and obtain a better behaviour of the receiver two crossovers have been implemented. The results are similar to the previous case and the improvement is not compensated by the complexity added to the receiver design. It has been recommended not making more than one crossover in the receiver.

Acknowledgements

The authors would like to thank the financial support of the Spanish government for the project ENE2012-34255.

References

Abe, O., Utsunomiya, T., Hoshino, Y., 1984. The thermal stability of binary alkali metal nitrates. Thermochim. Acta 78, 251–260. doi:10.1016/0040-6031(84)87150-6

Aicher, T., Martin, H., 1997. New correlations for mixed turbulent natural and forced convection heat transfer in vertical tubes. Int. J. Heat Mass Transf. 40, 3617–3626. doi:10.1016/S0017-9310(97)00026-4

American Society of Mechanical Engineers (ASME), 2011. ASME Boiler and Pressure Vessel Code, Section II - Materials. American Society of Mechanical Engineers, New York.

Augsburger, G., Favrat, D., 2013. Modelling of the receiver transient flux distribution due to cloud passages on a solar tower thermal power plant. Sol. Energy 87, 42–52. doi:10.1016/j.solener.2012.10.010

Baharoon, D.A., Rahman, H.A., Omar, W.Z.W., Fadhl, S.O., 2015. Historical development of concentrating solar power technologies to generate clean electricity efficiently – A review. Renew. Sustain. Energy Rev. 41, 996–1027. doi:10.1016/j.rser.2014.09.008

Cheesewright, R., Heggs, P.J., Martin, B.W., Parry, W.J., Ralston, T., 2001. Forced convection heat transfer in straight tubes. Part 2: laminar and transitional flow. London.

Collado, F.J., 2009. Preliminary design of surrounding heliostat fields. Renew. Energy 34, 1359–1363. doi:10.1016/j.renene.2008.09.003

Collado, F.J., Gómez, A., Turégano, J.A., 1986. An analytic function for the flux density due to sunlight reflected from a heliostat.pdf. Sol. Energy 37, 215–34.

Collado, F.J., Guallar, J., 2013. A review of optimized design layouts for solar power tower plants with campo code. Renew. Sustain. Energy Rev. 20, 142–154. doi:10.1016/j.rser.2012.11.076

Falcone, P.., 1986. A handbook for solar central receiver design. Sandia National Laboratories, Livermore, California.

Golden, C., 2015. System Advisor Model (SAM) [WWW Document]. Natl. Renew. Energy Lab. URL sam.nrel.gov/content/downloads (accessed 2.19.15).

Kistler, B.L., 1986. A User's Manual for DELSOL3: A Computer Code for Calculating the Optical Performance and Optimal System Design for Solar Thermal Central Receiver Plants. Albuquerque.

Kolb, G.J., 2011. An Evaluation of Possible Next-Generation High-Temperature Molten-Salt Power Towers. Alburquerque and Livermore, SAND20011-9320. doi:SAND20011-9320

Kolb, G.J., Ho, C.K., Mancini, T.R., Gary, J.A., 2011. Power Tower Technology Roadmap and Cost Reduction Plan. Sandia National Laboratories, Albuquerque.

Lata, J.M., Rodríguez, M., Álvarez de Lara, M., 2008. High Flux Central Receivers of Molten Salts for the New Generation of Commercial Stand-Alone Solar Power Plants. J. Sol. Energy Eng. 130, 1–5. doi:10.1115/1.2884576

Modest, F.M., 2003. Radiative Heat Transfer, in: Science, E. (Ed.), Radiative Heat Transfer. New York, San Francisco, London, pp. 162–197.

Nissen, D. a., Meeker, D.E., 1983. Nitrate/Nitrite Chemistry in NaN03-KN03 Melts. Inorg. Chem. 22, 716–721.

Pacheco, J.E., Ralph, M.E., Chavez, J.M., 1995. Investigation of Cold Filling Receiver Panels and Piping in Molten-Nitrate-Salt Central-Receiver Solar Power Plants. J. Sol. Energy Eng. 117, 282. doi:10.1115/1.2847839

Petukhov, B.S., 1970. Heat Transfer and Friction in Turbulent Pipe Flow with Variable Physical Properties. Moscow (USSR). doi:10.1016/S0065-2717(08)70153-9

Pugh, S.J., Garvey, S.J., 1993. Forced convection heat transfer in straight tubes. London, ESDU 92003.

Rodríguez-Sánchez, M.R., Marugan-Cruz, C., Acosta-Iborra, A., Santana, D., 2014a. Comparison of simplified heat transfer models and CFD simulations for molten salt external receiver. Appl. Therm. Eng. 73, 991–1003. doi:10.1016/j.applthermaleng.2014.08.072

Rodríguez-Sánchez, M.R., Soria-Verdugo, A., Almendros-Ibáñez, J.A., Acosta-Iborra, A., Santana, D., 2014b. Thermal design guidelines of solar power towers. Appl. Therm. Eng. 63, 428–438. doi:10.1016/j.applthermaleng.2013.11.014

Sánchez-González, A., Santana, D., 2015. Solar flux distribution on central receivers: a projection method from analytic function. Renew. Energy 74, 576–587.

Sánchez-González, A., Santana, D., 2015. Solar flux distribution on central receivers: A projection method from analytic function. Renew. Energy 74, 576–587. doi:10.1016/j.renene.2014.08.016

Siebers, D.L., Kraabel, J.S., 1984. Estimating convective energy losses from solar central receivers, SAND84-8717. Sandia National Laboratories, Livermore, CA.

Slusser, J.W., Titcomb, J.B., Heffelfinger, M.T., Dunbobbin, B.R., 1985. Corrosion in Molten Nitrate-Nitrite Salts. J. Met. 37, 24–27.

US Department of Energy, 2013. EnergyPlus Energy Simulation Software [WWW Document]. URL apps1.eere.energy.gov/buildings/energyplus/energyplus_about.cfm (accessed 2.25.15).

Vant-Hull, L.L., 2002. The Role of “Allowable Flux Density” in the Design and Operation of Molten-Salt Solar Central Receivers. J. Sol. Energy Eng. 124, 165. doi:10.1115/1.1464124

Wagner, M.J., 2008. Simulation and Predictive Performance Modeling of Utility-Scale Central Receiver System Power Plants. University of Wisconsin, Madison.

Winter, C.J., Sizmann, R.L., Vant-Hull, L.L., 1991. Solar Power Plants. Springer Berlin Heidelberg, Berlin, Heidelberg. doi:10.1007/978-3-642-61245-9

Zavoico, A.B., 2001. Solar Power Tower: Design Basis Document. San Francisco, SAND2001-2100.